A Study of Early Afterdepolarizations in Human Ventricular Tissue

Nele Vandersickel, Alexander V Panfilov

Department of Physics and Astronomy, Ghent University, Ghent, Belgium

Abstract

Early afterdepolarizations (EADs) are additional small amplitude spikes during the repolarization phase of the action potential. The presence of EADs strongly correlates with the onset of dangerous cardiac arrhythmias. Most in silico studies target various mechanisms of EAD formation and are mainly performed in animal models of cardiac cells and at a single cell level. However, most EAD-related cardiac arrhythmias feature complex spatial organization. Here, we first present our recent studies on 2D spatial wave patterns in models of human ventricular tissue with EAD-shaped action potentials. Next, we report on our first steps in studies of EAD-related arrhythmias in an anatomically accurate model of the human heart. For these studies, we use a TP06 model modified to mimic the effect of certain drugs. We show that from the initial conditions representing normal excitation of the heart, we can obtain two types of complex spatial patterns of excitation: (1) of the re-entrant type produced by Ca waves and mainly manifested as a complex focal activity on the surface of the heart, due to transmural filament orientation. For a more reduced repolarizaiton reserve, we also obtain (2) complex spatial oscillatory patterns of excitation.

1. Introduction

Heart beat is initiated by an electrical wave of excitation, which propagates through the cardiac tissue and initiates cardiac contraction. Abnormal excitations of the heart result in life-threatening cardiac arrhythmias. Sudden cardiac death due to ventricular fibrillation accounts for more than 400,000 deaths per year in the United States alone [1]. Understanding the mechanisms of initiation of cardiac arrhythmias is one of the most important problems in basic cardiology.

There are several factors shown to increase the probability of arrhythmia onset. One is the presence of EADs [2,3]. In normal situations, the repolarization of action potential during phases 2 and 3 is monotonous. In the case of EADs, there is a reversal of the action potential before the completion of its repolarization. EADs are found in many forms of long QT syndrome and also occur as side effects of some drugs, many of which were even not designed for heart disease [4]. In many cases, the presence of EADs is related to the onset of cardiac arrhythmias, including torsades de pointes (TdP) [4].

The mechanisms of onset of EADs at a single cell level have been addressed in many modeling studies. For example, the mechanisms of EAD generation and their rate dependency were studied in a guinea-pig cell model [5, 6]. These and other studies demonstrated that EADs occur as a result of decreases in the repolarization reserve, that can be achieved either by increasing the inward currents or decreasing the outwards currents [4]. A detailed study of EAD onset in the LR1 model with a wide range of parameters accounting for L-type Ca current was performed by [7]. This study showed that with a reduction of the repolarization reserve, typical action potential morphology changes from a normal action potential shape to EADs, and then to non-repolarizing action potential.

However, as cardiac arrhythmias mainly occur at the tissue or whole organ level, it is extremely important to study which spatial excitation patterns can be expected in tissues with cells showing EAD dynamics. Also, most previous studies were performed using models of animal cells. The aim of this paper is to review previous studies on EAD-induced excitation patterns in models of human ventricular tissue and present new results regarding the manifestation of these patterns in an anatomical model of the human heart.

2. Model and Numerical Methods

We use the following monodomain description [10] of cardiac tissue:

$$C_m \frac{\partial V_m}{\partial t} = \left(\frac{\partial}{\partial x_i} D_{ij} \frac{\partial V_m}{\partial x_j} \right) - I_{\text{ion}} \ , \qquad (1)$$

where D_{ij} is a diffusion matrix accounting for anisotropy of cardiac tissue, $i, j = 1...3$, C_m is membrane capacitance, V_m is transmembrane voltage, t is time, and I_{ion} is the total transmembrane ionic current given by the TP06 of human ventricular cardiomyocyte [8, 9] and is the sum of the following ionic currents:

$$I_{ion} = I_{Na} + I_{K1} + I_{to} + I_{Kr} + I_{Ks} + I_{CaL} + I_{NaCa} \quad (2)$$

$$+I_{NaK} + I_{pCa} + I_{pK} + I_{bCa} + I_{bNa} \quad (3)$$

The diffusion tensor is given by

$$D_{ij} = (D_L - D_T)\tau_i\tau_j + D_T\delta_{ij} \ , \quad (4)$$

with δ_{ij} the Kronecker symbol and τ_i a unit vector along cardiac fibers.

For anatomical modeling of the human ventricles we used the approach [11] with $D_L = 0.154mm^2/ms$ and $D_T = 1/4D_L$.

We used a finite difference approach with 18 points of discretization:

$$\frac{\tilde{V}_{ij} - V_{ij}}{\Delta t} = \frac{1}{\Delta x^2}\sum_{i'j'} w^{ij}_{i'j'} V_{i+i',j+j'} - Iion\left(V_{ij}, \ldots\right), \quad (5)$$

where Δt is the time step, Δx is the space step, and $w^{ij}_{i'j'}$ are the weights corresponding to the diffusion tensor at location i, j. For the gating variables, the Rush and Larsen method was used. The model was implemented in C++ using the CUDA toolkit for offloading the computations to the graphics cards. The program was run on an Intel Core i7-3930K machine with two NVIDIA GTX 780 graphics cards. A typical simulation of 1 sec of wave propagation in the heart requires 13.5 CPU min.

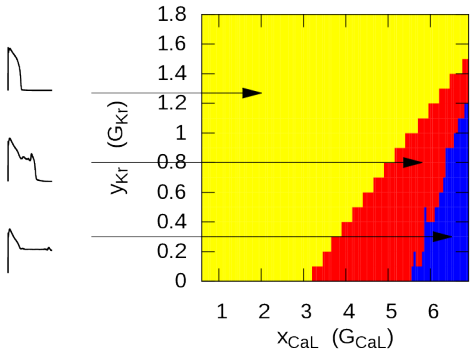

Figure 1. Parametric space of different AP behavior in TP06 model for human ventricular cells. The numbers on the x axis give the multiplication factor for the maximal calcium conductance, the y axis for the maximal conductance of I_{Kr}. Yellow, red, and blue colors indicate regions in which the AP has no EAD, the AP appears with EADs, and the AP does not return to the resting potential, respectively.

3. 2D excitation patterns in EAD-prone tissue

Before we consider excitation patterns in the anatomical model of the heart, let us consider possible patterns which occur in 2D tissue.

In [12–14], we studied spatial manifestations of EAD patterns in two models of human ventricular tissue. To obtains EADs, we have changed the balance between the inward currents and outward currents. In particular, we increased the value of ICaL or NCx and decreased the values of the potassium currents (IKr or IKs). These changes mimic the application of isoproterenol [5] and potassium channel blockers [15], which are known promoters of EADs.

Figure 1 shows plots of possible action potential shapes that occur if ICaL is progressively increased and IKr is progressively decreased. We see that we have a progressive change of the patterns from normal action potential, to single EAD responses, and then to non-repolarizing triggered activity with small amplitude oscillations.

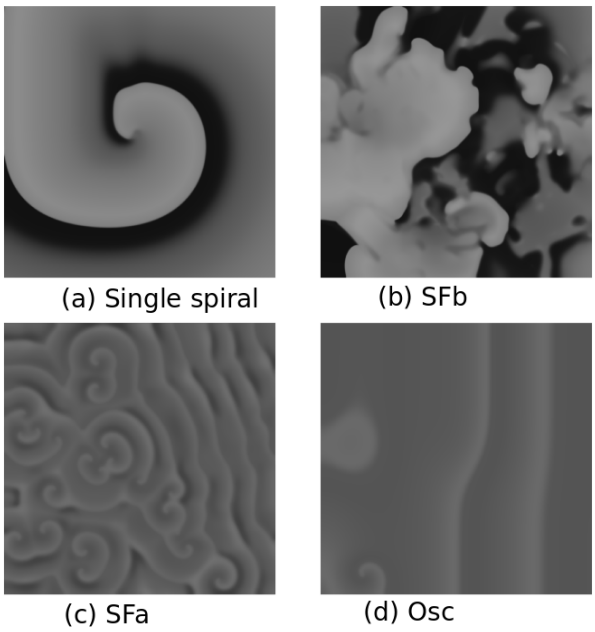

Figure 2. Illustration of the different types of fibrillation induced by EADs. In Figure (a), a single spiral is shown for standard parameters, (b) SFb for parameters $3.5 \times G_{CaL}$, $0.9 \times G_{Kr}$, (c) SFa for parameters $4 \times G_{CaL}$, $0 \times G_{Kr}$ and (d) the oscillatory pattern for parameters $5 \times G_{CaL}$, $0.1 \times G_{Kr}$.

When we considered spatial dynamics in 2D tissue that occur as the result of such single cell activity, we found the three main types of dynamics illustrated in Figure 2.

For the initial conditions in the form of a single spiral

wave, we can observe either normal situation: the spiral wave remains intact (Figure 2a) or it can decay into complex spatio-temporal patterns, which we call fibrillation. We found three different types of fibrillation. In the first type, the wavefront is mediated by both INa and ICaL currents, and the pattern consists of chaotic, unstable spiral waves (Figure 2b). In the second type, the wavefront is driven by ICaL and the pattern comprises stable and unstable spirals, which have a much more distinct spiral shape and are more persistent than those from type 1. The third type of excitation patterns may consist of spirals or point sources, which may have a complex spatial shape. The wavefronts are driven by ICaL; however, the observed waves here are phase waves, which, for example, cannot be removed by placing multiple barriers to the tissue [12]. We have also found that the onset of EADs dramatically increases the threshold of defibrillation [13], and in the case of substantial decrease of the repolarization reserve, defibrillation even becomes impossible. We have also found [14] that the same types of excitation patterns are not restricted by the TNNP/TP06 model, but they also occur in the ORd model for human ventricular tissue [16].

Here, we extend our studies to an anatomically accurate model of human ventricles and study the possible types of excitation patterns that can be observed there.

4. Excitation patterns in EAD-prone tissue in an anatomical mode of human ventricles

Figures 3 and 4 show typical excitation patterns that occur in an anatomically accurate model of the ventricles of the human heart. For better representation of wave dynamics we show the results of these 3D simulations on a 2D slice close to the base of the heart. We considered homogeneous tissue and, as in 2D simulations, progressively decreased the repolarization reserve through an increase of I_{CaL} and a decrease of I_{Kr}. We initiated waves on the endocardial side of the heart, similar to normal cardiac excitation, and we studied how EAD formation can lead to VF. Figure 3 shows the typical excitation pattern that we obtained for the parameter value $4 \times G_{CaL}$, $0.1 \times G_{Kr}$. This pattern is equivalent to SFa type VF, shown in 2D in Figure 2c. We observed many short-lived Ca-mediated scroll waves inside the heart (see Figure 3b). The scrolls were short-lived as they collided with each other and the boundaries of the heart. At the same time, new scroll waves were constantly formed.

On the surface of the heart, such excitation patterns gave rise to focal activity. This was because the filaments of the scroll waves did not exit to the epicardial surface and were mainly intramural. In a few cases, we have also observed long-lived Ca-mediated spirals on the surface of the heart.

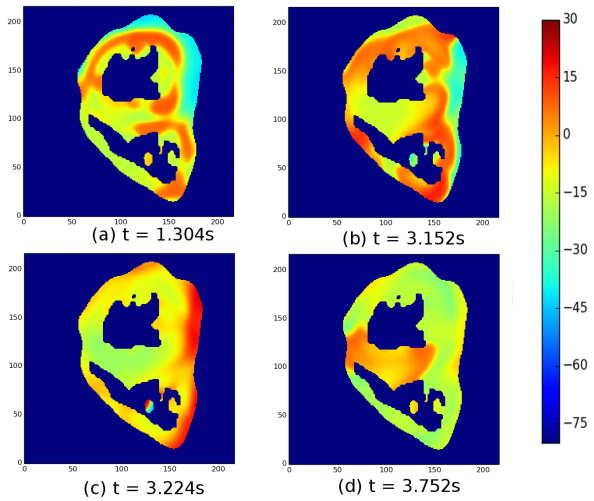

Figure 3. SFa in the whole heart; a spiral wave can be observed in Figure (b), which was short-lived. Simulations in 3D anatomically accurate model of the human ventricles. Excitation is shown on a slice close to the base of the heart. The parameter values for this simulation were $4 \times G_{CaL}$, $0.1 \times G_{Kr}$.

However, surface focal activity was a dominating spatial pattern. When I_{CaL} was further increased to 4.5 times its original value, we observed the oscillatory type (Figure 4). In this case, focal activity seemed to originate from the endocardial side of the heart (Figure 4a and 4d). Of course, in this case the surface manifestation of such activity was also of the focal type. This excitation pattern is similar to the 2D oscillatory pattern shown in Figure 2d. As shown in 2D [12, 14], such oscillatory patterns are formed by phase waves. Therefore, we suggest that the patterns shown in Figure 4 are produced by phase waves as well. Another wave pattern found in our 2D simulation was VF of the SFa type. Thus far, we have not observed such patterns in whole heart simulations. This is because the generation of an SFa pattern requires initial conditions in the form an existing spiral wave. We plan to extend our studies to these initial conditions and expect to find and characterize VF of the SFa type in an anatomical model of the heart in the near future.

Acknowledgements

This research is supported by the Research-Foundation Flanders (FWO Vlaanderen and by the BOF of Ghent University.

References

[1] Go AS, Mozaffarian D, Roger VL, Benjamin EJ, Berry JD, Borden WB, Bravata DM, Dai S, Ford ES, Fox CS,

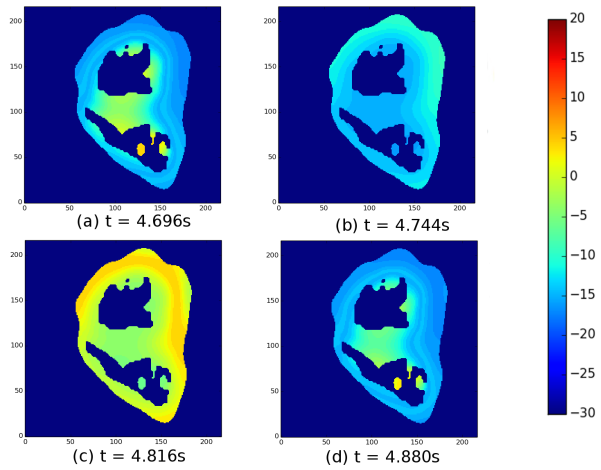

Figure 4. Oscillatory pattern in the whole heart for the parameter value $4.5 \times G_{CaL}$, $0.1 \times G_{Kr}$.
Simulations in 3D anatomically accurate model of the human ventricles. Excitation is shown on a slice close to the base of the heart.

Franco S, Fullerton HJ, Gillespie C, Hailpern SM, Heit JA, Howard VJ, Huffman MD, Kissela BM, Kittner SJ, Lackland DT, Lichtman JH, Lisabeth LD, Magid D, Marcus GM, Marelli A, Matchar DB, McGuire DK, Mohler ER, Moy CS, Mussolino ME, Nichol G, Paynter NP, Schreiner PJ, Sorlie PD, Stein J, Turan TN, Virani SS, Wong ND, Woo D, Turner MB. Heart disease and stroke statistics2013 update. A report from the American Heart Association. Circulation 2012; 127: e6–e245.

[2] Cranefield PF Action potentials, afterpotentials, and arrhythmias. Circ Res 1997; 41: 415–423.

[3] Qu Z, Xie LH, Olcese R, Karagueuzian HS, Chen PS, Garfinkel A, Weiss J.N. Early afterdepolarizations in cardiac myocytes: Beyond reduced repolarization reserve. Cardiovasc Res. 2013: 99 :6–15

[4] Roden DM, Viswanathan PC Genetics of acquired long qt syndrome. J Clin Invest 2005; 115: 2025–2032.

[5] Zeng J, Rudy Y Early afterdepolarizations in cardiac myocytes: mechanism and rate dependence. Biophys J. 1995; 68: 949–964.

[6] Clancy CE, Rudy Y Linking a genetic defect to its cellular phenotype in a cardiac arrhythmia. 1999;Nature 400: 566–569.

[7] Tran DX, Sato D, Yochelis A, Weiss JN, Garfinkel A, et al. Bifurcation and chaos in a model of cardiac early afterdepolarizations. Phys Rev Lett. 2009; 102: 258103.

[8] ten Tusscher KH, Noble D, Noble PJ, Panfilov AV A model for human ventricular tissue. Am J Physiol Heart Circ Physiol 2004; 286: H1573–1589.

[9] ten Tusscher KH, Panfilov AV Alternans and spiral breakup in a human ventricular tissue model. Am J Physiol Heart Circ Physiol 2006; 291: H1088–1100.

[10] Keener JP, Sneyd J. Mathematical Physiology. New York: Springer-Verlag, 1998.

[11] ten Tusscher KH, Hren R, Panfilov AV. Organization of ventricular fibrillation in the human heart. Circ Res 2007;100: 87–101.

[12] Vandersickel N, Kazbanov IV, Nuitermans A, Weise LD, Pandit R, Panfilov AV. A study of early afterdepolarizations in a model for human ventricular tissue. PLoS One. 2014; 9:e84595

[13] Vandersickel N, Kazbanov IV, Defauw A, Pijnappels DA, Panfilov AV. Decreased repolarization reserve increases defibrillation threshold by favoring early afterdepolarizations in an in silico model of human ventricular tissue. Heart Rhythm. 2015; 12:1088–1096.

[14] Zimik S, Vandersickel N, Nayak AR, Panfilov AV, Pandit R. A Comparative Study of Early Afterdepolarization-Mediated Fibrillation in Two Mathematical Models for Human Ventricular Cells. PLoS One. 2015; 10:e0130632.

[15] Asano Y, Davidenko JM, Baxter WT, Gray RA, Jalife J (1997) Optical mapping of drug-induced polymorphic arrhythmias and torsade de pointes in the isolated rabbit heart. J Am Coll Cardiol 1997;29: 831–842.

[16] OHara T, Virg L, Varr A, Rudy Y. Simulation of the undiseased human cardiac ventricular action potential: model formulation and experimental validation. PLoS computational biology. 2011; 7(5): e1002061

Address for correspondence:

Alexander V. Panfilov
Department of Physics and Astronomy, Ghent University, Krijgslaan 281, S9, Ghent, 9000 Belgium
E-mail:Alexander.Panfilov@UGent.be